A PHYSICS-BASED MODEL FOR ACTIVE CONTOURS: A COMPUTATIONAL ALGEBRAIC TOPOLOGY APPROACH

P. Poulin [a], M.-F. Auclair-Fortier [a], D. Ziou [a], M. Allili [b]

[a] Groupe de Moivre, Département de mathématiques et d'informatique, Université de Sherbrooke, Sherbrooke, Québec, J1K 2R1, Canada - (poulin, auclair, ziou)@dmi.usherb.ca

[b] Depts. of Comp. Sc. And Math., Bishop's University, Lennoxville, Québec, J1M 1Z7, Canada – mallili@ubishops.ca

KEY WORDS: Curve Deformation, Partial Differential Equations, Physical Laws, Computational Algebraic Topology, Active Contours, Shape-Based Image Retrieval

ABSTRACT:

We present a new method for the deformation of curve based upon a decomposition of the elasticity problem into basic physical laws. We encode the basic laws using computational algebraic topology. Each basic law uses exact global values and makes approximations only when they are needed. The deformations computed with our approach have a physical interpretation. Furthermore, our algorithm performs with either 2D or 3D problems. We finally present results validating our approach.

1. INTRODUCTION

The main problem addressed in this paper concerns the deformation of curves for which several methods have been proposed (Gibson, and Mirtich, 1997, Montagnat, Delingette, Scapel and Ayache, 2000). Physics-based methods (Platt and Badler, 1981, Sclaroff and Pentland, 1995) and methods arising from variational calculus (Bentabet, Jodouin, Ziou and Vaillancourt, 2001, Kass, Witkin, and Terzopoulos, 1987) have been considered to control the deformations.

The numerical solutions obtained with the existing techniques do not always have a physical interpretation. Those arising from variational calculus are usually based upon purely mathematical techniques. In this paper, we propose a new model which includes a physical interpretation of the deformations and offers a systematic method for reflecting some properties of the materials. It also proposes to use exact global values valid over a region instead of considering only local ones. To achieve it, we directly use the physical laws governing the deformations and encode them using a computational algebraic topology (CAT)-based image model. This model makes use of chains, boundaries, cochains and coboundaries to represent the image support and the quantities defined over it.

Our approach has several important advantages. 1) Since the linear elasticity problem is well-known in continuum mechanics then our modelling can be performed wisely and provide some good physical interpretation of the whole de-formation process and of its intermediate steps. 2) The use of global values leads to an algorithm which is less sensitive to noise. 3) The use of coboundaries to link the field quantities defined over pixels of different dimensions provides a modular computational scheme easy to reproduce. The coboundaries are defined according to the suitable basic laws prescribed by each problem. 4) Thanks to the modularity, the approach can easily be generalized to surfaces and volumes.

The approach has been validated in the context of the correction of synthetic and real images of road databases. In the following, and after decomposing the elasticity problem into basic laws, we summarize the CAT-based image model and propose a representation of the problem based upon it. This representation is then used to compute the regularization constraints which are employed to control the deformations. Applications and experimental results are then presented.

2. DECOMPOSITION INTO BASIC LAWS

The first basic laws which are relevant to us are the well-known strain-displacements relations (Poulin, Auclair-Fortier, Ziou, and Allili, 2001):

$$\varepsilon_{ij} = \frac{1}{2}\left[\frac{\partial u_i}{\partial x_j} + \frac{\partial u_j}{\partial x_i}\right] \qquad (i, j = 1,2,3) \qquad (1)$$

where u_i is the change in length of the original body in the direction of $\boldsymbol{x_i}$.

Our next basic laws concern the force-stress relation. Given distributed body forces ρb_i and traction forces $t_i^{\boldsymbol{n}}$ applied to a body moving under the velocity field $v_i = v_i(\boldsymbol{x}, t)$, the principle of linear momentum (Boresi, 1965) states that the resultant force acting on a body is equal to the rate of change over time of the linear momentum. Thus

$$\frac{d}{dt}\iiint_V \rho v_i \, dV \quad = \quad \iint_S t_i^{\boldsymbol{n}} \, dS + \iiint_V \rho b_i \, dV \qquad (2)$$

lin. momentum = Forces acting on the body

Using the Cauchy stress formula (Mase and Mase, 1999) :

$$t_i^{\boldsymbol{n}} = \sum_{j=1}^{3} \sigma_{ji} n_j \qquad (3)$$

and Gauss's divergence theorem, we have

$$\frac{d}{dt}\iiint_V \rho v_i dV = \iiint_V (\nabla \cdot \sigma_i + \rho b_i) dV \qquad (4)$$

where $\sigma_i=(\sigma_{1i},\sigma_{2i},\sigma_{3i})^T$ and σ_{ij} is the stress component in the direction of x_j when the unit normal vector $\boldsymbol{n}=(n_1,n_2,n_3)^T$ is parallel to x_i. Since the element of volume is arbitrary then the integral sign can be taken off and the second basic laws, also known as the equilibrium equations, are obtained assuming a zero velocity field in Eq.4:

$$\nabla \cdot \sigma_i = \rho b_i \qquad (5)$$

In order to explain how the internal forces of an elastic body vary when it undergoes deformations, we must take into account a constitutive equation (or material law) which reflect the internal constitution of the materials. Our last basic law is known as the generalized Hooke's law for linear elastic isotropic materials in plane strain situations (Mase and Mase, 1999) and is given by the following equations:

$$\sigma_{ii} = \frac{\mathrm{E}}{(1+\nu)(1-2\nu)}\left[(1-\nu)\varepsilon_{ii} + \nu(\varepsilon_{jj} + \varepsilon_{kk})\right] \qquad (6)$$

$$\sigma_{ij} = 2G\varepsilon_{ij} = \frac{\mathrm{E}}{(1+\nu)}\varepsilon_{ij} \qquad (i \neq j) \qquad (7)$$

where E is the modulus of elasticity of Young, ν the Poisson ratio and $G = \dfrac{E}{2(1+\nu)}$ the modulus of rigidity.

3. ENCODING OF THE BASIC LAWS USING THE CAT-BASED IMAGE MODEL.

An image is composed of two distinctive parts: the image support (pixels) and some field quantity associated with each pixel. This quantity may be scalar (e.g. grey level), vectorial (e.g. force) or tensorial (e.g. Hessian). We model the image support in terms of cubical complexes, chains and boundaries. For quantities, we introduce the concept of cochains which are representations of fields over a cubical complex. A detailed version of the CAT-based image model and some applications in image processing may be found in (Auclair-Fortier, Poulin, Ziou and Allili, 2001, Poulin, Auclair-Fortier, Ziou and Allili, 2001, Ziou and Allili, 2001).

To encode the basic laws of the elasticity problem, the image support is subdivided into cubical complexes. Then global quantities are computed over -pixels via cochains according to basic laws. The constitutive equations 6 and 7 are expressed as linear transformations between two cochains. Since we want to represent two kinds of global values over the image, we use two complexes. The first complex is associated with variables describing the configuration of the system (e.g. displacements) while the second complex refers to the source variables (e.g. forces) (Tonti, 2001).

The first laws (Eq. 1) are modeled as 1-cochains $< \mathcal{D},\ \gamma_D >$ for a 1-pixel γ_D over a 3-complex $\mathcal{K}^p$ with $\partial\gamma_D = x^* - x^\#$. Considering the normal strains ε_{11}, ε_{22} and ε_{33} in Eq.1 we have an application ε

$$\begin{aligned} \varepsilon\colon \mathbb{R}^3 &\to \mathbb{R}^3 \\ \mathbf{U} &\mapsto \varepsilon(\mathbf{U}) = (\varepsilon_{11}, \varepsilon_{22}, \varepsilon_{33})^T = \nabla\mathbf{U} \end{aligned} \qquad (8)$$

Let us define the cochain $\mathcal{D}$ as

$$< \mathcal{D},\ \partial\gamma_D > = \int_{\gamma_D} \varepsilon(\mathbf{U}) d\gamma_D \qquad (9)$$

Let us apply a 0-cochain $\mathcal{U}$ to $\partial\gamma_D$

$$< \mathcal{U},\ \partial\gamma_D > = \mathcal{U}(\boldsymbol{x}_* - \boldsymbol{x}_\#) = \mathcal{U}(\boldsymbol{x}_*) - \mathcal{U}(\boldsymbol{x}_\#)$$

and use the line integral theorem in Eq.9. Then we have

$$< \mathcal{D},\ \partial\gamma_D > = \mathbf{U}(\boldsymbol{x}_*) - \mathbf{U}(\boldsymbol{x}_\#)$$

We thus define $\mathcal{U}(\boldsymbol{x}) = \mathbf{U}(\boldsymbol{x})$. The cochain $\mathcal{D}$ is then the coboundary of $\mathcal{U}$.

The second laws (Eq. 5) are modelled as 3-cochains $< \mathcal{F},\ \gamma_F >$ for a 3-pixel γ_F over a 3-complex $\mathcal{K}^S$

$$< \mathcal{F},\ \gamma_F > = \int_{\gamma_F} \nabla \cdot \sigma_i d\gamma_F$$

Applying the divergence theorem to $\mathcal{F} = (\mathcal{F}_1, \mathcal{F}_2, \mathcal{F}_3)^T$, we have

$$< \mathcal{F}_i, \gamma_F > = \sum_{\gamma_{S_j} \in \partial_{\gamma_F}} \sigma_i \cdot n_j d\gamma_{S_j} \qquad (10)$$

where $\boldsymbol{n}_j$ is the normal vector to γ_{S_j}. Then we define a 2-cochain $\mathcal{S} = (S_1, S_2, S_3)^T$ such that

$$< S_i, \gamma_{S_j} > = \int_{\gamma_{S_j}} \rho_i \cdot n_j d\gamma_{S_j} \qquad (11)$$

Then the cochain $\mathcal{F}$ is the coboundary of $\mathcal{S}$.

We finally need to represent the Hooke's law (Eqs 6 and 7) which links the local values of $\varepsilon(\boldsymbol{x})$ and $\sigma(\boldsymbol{x})$. In cochain terms, we want to link the cochains $\mathcal{D}$ and $\mathcal{S}$. Since Eqs 6 and 7 are constitutive equations, we cannot provide a topological expression of them. We use a piecewise approximation) and $\tilde{\mathbf{U}}(\boldsymbol{x})$ of $\mathbf{U}(\boldsymbol{x})$ such that for each 1-face γ_D of a 2-pixel γ of $\mathcal{K}^p$ we have

$$\int_{\gamma_D} \tilde{\varepsilon}(\boldsymbol{x}) d\gamma_D = < D, \gamma_D > \qquad (12)$$

Applying the generalized Hooke's law to $\tilde{\varepsilon}(\mathbf{x})$ satisfying Eq. 12, we have

$$\tilde{\sigma}_{ii}(\boldsymbol{x}) = \mathrm{E}\left[\frac{(1-\nu)\tilde{\varepsilon}_{ii}(\boldsymbol{x}) + \nu\left(\tilde{\varepsilon}_{jj}(\boldsymbol{x}) + \tilde{\varepsilon}_{kk}(\boldsymbol{x})\right)}{(1+\nu)(1-2\nu)}\right]$$

$$\tilde{\sigma}_{ij}(\boldsymbol{x}) = \frac{\mathrm{E}}{(1+\nu)}\tilde{\varepsilon}_{ij}(\boldsymbol{x}) \qquad (i,j = 1,\ 2,\ 3)(i \neq j)$$

at all point $\boldsymbol{x}$ of γ. Eq. 11 is then replaced by

$$< S_j, \gamma_{S_j} > = \iint_s \tilde{\sigma}_i(\boldsymbol{x}) \cdot n dS \qquad (i = 1,\ 2,\ 3) \quad (13)$$

which depends on the choice of the approximation function $\tilde{\varepsilon}(\boldsymbol{x})$.

4. APPLICATION

We apply our approach to a 2D active contours model based upon a Lagrangian evolution of a curve S

$$\frac{\partial S}{\partial t} + \mathbf{K}S = \mathbf{F}_{\text{ext}}(S) \qquad (14)$$

where $\mathbf{K}$ is a matrix computed with the basic laws of Section 2 and encoding the regularizing constraints. Assuming that the initial curve S_0 was in an equilibrium state and that the initial body forces $\mathbf{F_0} = \mathbf{K}S_0$ are constant during the deformation process, we can add these forces to the external forces $\mathbf{F}_{\text{ext}}$ and solve Eq. 14 with an explicit scheme

$$S_{t+\Delta t} = S_t + \Delta t\left(\mathbf{F}_{\text{ext}} - \mathbf{K}\mathbf{U}_t\right) \qquad (15)$$

where $\mathbf{U}_t$ is the displacement vector for the curve S at t.

We want to solve Eq. 15 for local $\mathbf{U}(\boldsymbol{x})$ located at the center of each pixel and known initial curve S_0 close to the solution. To achieve it, we first position the two cubical complexes $\mathcal{K}^p$ and $\mathcal{K}^S$ such that the 0-pixels of $\mathcal{K}^p$ correspond to the center of the image pixels the 2-pixels of $\mathcal{K}^S$ coincide with the image pixels. This way of positioning $\mathcal{K}^S$ allows the use of an approximation polynomial of order 1 with the same accuracy as that obtained using one of order 2 (Mattiussi, 1997).

In order to solve Eq. 15, we need global values $\mathbf{F}_{\text{ext}}$ over each pixel of $\mathcal{K}^S$. Since these values are generally known, we did not try to express them in a topological way in the last section. In our examples, we use the line plausibility image obtained using a line detector proposed by Ziou (Ziou, 2000).

We then choose an approximation function $\tilde{\varepsilon}(\boldsymbol{x}) = (\tilde{\varepsilon}_{11}(\boldsymbol{x}), \tilde{\varepsilon}_{22}(\boldsymbol{x}))^T$. For simplicity, we assume that $\tilde{\varepsilon}(\boldsymbol{x}) = \nabla\tilde{\mathbf{U}}(\boldsymbol{x})$ arises from a bilinear approximation of $\mathbf{U}(\mathbf{x})$ and that it satisfies Eq. 12. Then for a 2-pixel of $\mathcal{K}^p$ (Fig. 1), we have

$$\tilde{\varepsilon}(\boldsymbol{x}) = \left[\frac{D_1}{\Delta} + \frac{D_3 - D_1}{\Delta^2}x_2,\ \frac{D_4}{\Delta} + \frac{D_4 - D_2}{\Delta^2}x_1\right]^T \qquad (16)$$

In order to compute the cochain $< \mathcal{F}, \gamma_F >$, we use four approximation functions $\tilde{\sigma}_i^a$, $\tilde{\sigma}_i^b$, $\tilde{\sigma}_i^c$ and $\tilde{\sigma}_i^d$ because each γ_F intersects four 2-pixels of $\mathcal{K}^p$, (see Fig. 2). We find the value of the cochain over the four 1-faces of γ_F using Eq. 11:

$$S_i^1 = \int_0^{\frac{\Delta}{2}} \tilde{\sigma}_i^A\left(\frac{\Delta}{2}, x_2\right) \cdot \vec{\imath}\, dx_2 + \int_{\frac{\Delta}{2}}^0 \tilde{\sigma}_i^B\left(\frac{\Delta}{2}, x_2\right) \cdot \vec{\imath}\, dx_2$$

and so on for S_i^2, S_i^3 and S_i^4. Using Eq. 10 we have

$$< \mathcal{F}_i,\ \gamma_F > = S_i^1 + S_i^2 + S_i^3 + S_i^4 \qquad (17)$$

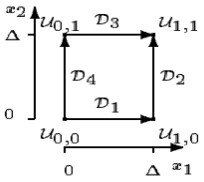

Figure 1. A 2-pixel of $\mathcal{K}^p$ and the topological quantities associated with it.

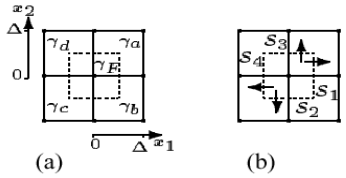

Figure 2. (a) γ_F in dashed lines (b) 2-cochain *S*.

Eq. 17 expresses the internal forces $\boldsymbol{F}_1$ and $\boldsymbol{F}_2$ as a function of the displacement **U**. As an example, we present the values of $\boldsymbol{F}_1$ and $\boldsymbol{F}_2$ for the 2-pixel γ_F of Fig. 1 with Δ=1:

$$\begin{aligned} F_1 = C\big[&(3-4\nu)u_{-1,1} + (2-8\nu)u_{0,1} + (3-4\nu)u_{1,1} \\ &+ (10-8\nu)u_{-1,0} + (-36+48\nu)u_{0,0} + (10-8\nu)u_{1,0} \\ &+ (3-4\nu)u_{-1,-1} + (2-8\nu)u_{0,-1} + (3-4\nu)u_{1,-1} \\ &- 2v_{-1,1} + 2v_{1,1} + 2v_{-1,-1} + -2v_{1,-1}\big] \end{aligned} \qquad (18)$$

$$\begin{aligned} F_2 = C\big[&(3-4\nu)v_{-1,1} + (10-8\nu)v_{0,1} + (3-4\nu)v_{1,1} \\ &+ (2-8\nu)v_{-1,0} + (-36+48\nu)v_{0,0} + (2-8\nu)v_{1,0} \\ &+ (3-4\nu)v_{-1,-1} + (10-8\nu)v_{0,-1} + (3-4\nu)v_{1,-1} \\ &- 2u_{-1,1} + 2u_{1,1} + 2u_{-1,-1} - 2u_{1,-1}\big] \end{aligned} \qquad (19)$$

where $C = \dfrac{E}{16(1+\nu)(1-2\nu)}$ and $\mathbf{U} = \begin{bmatrix} \mathbf{u} \\ \mathbf{v} \end{bmatrix}$.

Eqs 18 and 19 set a linear relationship between a pixel and its neighbors. This relation is used to build the stiffness matrix **K** of Eq. 15.

5. EXPERIMENTAL RESULTS

The proposed approach was first used to develop a shape-based image retrieval system (Poulin, Auclair-Fortier, Ziou and Allili, 2001). It was also tested in the context of the correction of high-resolution real and synthetic images of road databases. This section presents some results for this application. We compare the results obtained with our physics-based method (PBM) with those obtained with a finite element method (FEM) (Bentabet, Jodouin, Ziou and Vaillancourt, 2001).

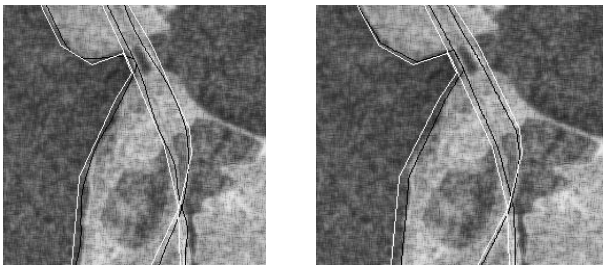

(a) FEM (b) PBM

Figure 3: Road corrections.

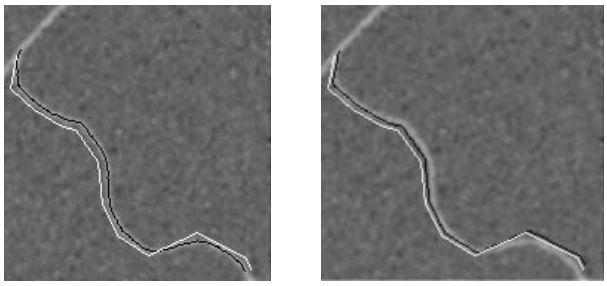

(a) (b)

Figure 4: Shape recovery of a curve when the image forces are taken off.

The first image is a section of a RADARSAT SAR image centered on the region of Stephenville (Québec), Canada* with a 25-meter resolution. In this image, the roads correspond to linear features. Figs 3(a) and 3(b) show respectively in black the results obtained with the PBM (E=200 and ν=0.45) and FEM (α=0.03 and β=137.8 for the most left curve). The initialization snake is drawn in white in both figures. One can notice that the PBM most left corrected curve is closer to the exact road than the FEM one in regions of high curvature.

The deformations modeled using the PBM have the interesting property of allowing the objects to recover their original shape when the image forces applied to them are taken off. To illustrate this fact, Fig. 4(a) presents a synthetic image in which the initial and corrected roads are respectively drawn in white and black. Fig. 4(b) shows respectively in black and white the corrected curve when the image forces are taken off and the initial snake. Since the initial body forces $\mathbf{F}_0$ are the only forces applied to the deformed curve, then it recovers its initial shape. However, one can show that the computation of the internal forces is invariant with respect to translation and then the curve can experience a spatial shift as in Fig. 4(b).

This paper presented a new model for the deformation of curves. The proposed approach makes use of both local and global values through a decomposition of the elasticity problem into basic physical laws. These laws are encoded by cochains over cubical complexes and linked together using coboundaries. The coboundary formalism is a generic one and then it leads to algorithms which can easily be extended to higher dimensions. The use of the basic laws provides a physical interpretation of the deformation process. This interpretation was used to develop an active contours model.

* The image was provided by the Canadian Space Agency under the ADRO-2 program.

ACKNOWLEDGEMENTS

This research was partly founded by the National Sciences and Engineering Research Council of Canada and by the Fonds Québécois de la Recherche sur la Nature et les Technologies. The authors also wish to thank Olivier Delalleau for his contribution in the understanding of the physical model.

REFERENCES

References from Journals:

Kass, M., Witkin, A. and Terzopoulos, D., 1987. Snakes: Active Contour Models. *International Journal of Computer Vision*, 1:321–331.

Mattiussi, C., 1997. An Analysis of Finite Volume, Finite Element, and Finite Difference Methods Using Some Concepts from Algebraic Topology. *Journal of Computational Physics*, 133:289–309.

Sclaroff, S. and Pentland, A., 1995. Modal Matching for Correspondance and Recognition. IEEE *Transactions on Pattern Analysis and Machine Intelligence*, 17(6):545–561.

Tonti, E., 2001. A Direct Discrete Formulation of Field Laws: The Cell Method. *CMES-Computer Modeling in Engineering & Sciences*, 2(2):237–258.

References from Books:

Boresi, A., 1965. *Elasticity in Engineering Mechanics*. Prentice-Hall.

Mase, G. T. and Mase, G. E., 1999. *Continuum Mechanics for Engineers*. CRC Press.

Platt, S. and Badler, N., 1981. Animating Facial Expressions. *Computer Graphics*, 15(3):245–252.

References from Other Literature:

Auclair-Fortier, M.-F., Poulin, P., Ziou, D. and Allili, M., 2001. A Physics-Based Resolution of Diffusion and Optical Flow: A Computational Algebraic Topology Approach. Technical Report 269, Département de mathématiques et d'informatique, Université de Sherbrooke.

Bentabet, L., Jodouin, S., Ziou, D., and Vaillancourt, J., 2001. Automated Updating of Road Databases from SAR Imagery: Integration of Road Databases and SAR Imagery information. information. In *Proceedings of the Fourth International Conference on Information Fusion*, volume WeA1, pp. 3–10.

Gibson, S. and Mirtich, B., 1997. A Survey of Deformable Modeling in Computer Graphics. Technical report, Mitsubishi Electric Research Laboratory.

Montagnat, J., Delingette, H., Scapel, N. and Ayache, N., 2000. Representation, Shape, Topology and Evolution of Deformable Surfaces. Application to 3D Medical Imaging Segmentation. Technical Report 3954, INRIA.

Poulin, P., Auclair-Fortier, M.-F., Ziou, D. and Allili, M., 2001. A Physics-Based Model for the Deformation of Curves: A Computational Algebraic Topology Approach. Technical Report 270, Département de mathématiques et d'informatique, Université de Sherbrooke.

Ziou, D., 2000. Optimal Line Detector. In *International Conference on Pattern Recognition (ICPR'00)*, Barcelona, SPAIN, September 3-8.

Ziou, D. and Allili, M., 2001. An Image Model with Roots in Computational Algebraic Topology: A Primer. Technical Report 264, Département de Mathématiques et d'informatique, Université de Sherbrooke.